

Sensitivity of a Global Ocean General Circulation Model to Tracer Advection Schemes

HIROYASU HASUMI AND NOBUO SUGINOHARA

Center for Climate System Research, University of Tokyo, Tokyo, Japan

6 August 1998 and 16 March 1999

ABSTRACT

Vertical diffusivity at the thermocline depths is now believed to be as small as $1 \times 10^{-5} \text{ m}^2 \text{ s}^{-1}$. In order to accomplish a reliable simulation of the World Ocean for the vertical diffusivity of $1 \times 10^{-5} \text{ m}^2 \text{ s}^{-1}$, two advective tracer transport schemes, the Uniformly Third-Order Polynomial Interpolation Algorithm (UTOPIA) of Leonard et al. and the Multidimensional Positive Definite Advection Transport Algorithm (MPDATA) of Smolarkiewicz, are incorporated into an ocean general circulation model. Intercomparison is made among simulations using UTOPIA, MPDATA, and the centered differencing scheme. When UTOPIA or MPDATA is adopted, features at the thermocline depths are realistically simulated. Increase in computational cost is moderate. Circulations associated with Antarctic Bottom Water (AABW) in the Atlantic and Circumpolar Deep Water (CDW) in the Pacific are not reproduced at all for such small vertical diffusivity, although the circulation associated with North Atlantic Deep Water (NADW) has reasonable intensity. Another experiment with UTOPIA for the vertical diffusivity of $5 \times 10^{-5} \text{ m}^2 \text{ s}^{-1}$ shows that the circulation associated with NADW is relatively insensitive to vertical diffusivity, compared with the circulation associated with AABW and CDW.

1. Introduction

Most OGCMs used so far adopt the centered differencing scheme for advective tracer transport (e.g., Bryan 1969). This scheme induces so-called numerical dispersion, which causes nonphysical spatial oscillation in the tracer field. When the vertical diffusion coefficient is taken sufficiently large, such nonphysical oscillation is damped to die out. As the vertical diffusion coefficient is taken smaller, however, such oscillation survives and causes unstable vertical stratification, especially where the vertical velocity is large (Yamanaka et al. 1999, manuscript submitted to *J. Phys. Oceanogr.*). Since OGCMs usually remove unstable vertical stratification by invoking convective adjustment (instantaneous vertical homogenization) or giving a highly enhanced value for the vertical diffusion coefficient, such oscillation leads to strong vertical mixing. In consequence, nonphysical structure appears in the result, or the computation blows up.

Some OGCMs adopt the upstream or the weighted upstream scheme for advective tracer transport (e.g., Maier-Reimer et al. 1993; Sugino-hara and Aoki 1991). These schemes do not induce nonphysical oscillation. Instead, their accuracy is lower than that of the centered

differencing scheme, and the effect of the error is to enhance diffusion. The diffusivity induced by such numerical diffusion is approximately proportional to the width of the numerical grid and the advection velocity. When we want to keep the numerical vertical diffusivity smaller than $1 \times 10^{-5} \text{ m}^2 \text{ s}^{-1}$, which is the observed value at thermocline depths (e.g., Gregg 1989; Ledwell et al. 1993), the vertical numerical grid spacing should be taken less than several meters. Such fine resolution requires enormous time in computation, thus making it difficult to carry out a global ocean simulation. The behavior of the centered differencing and the weighted upstream schemes in an OGCM is well documented by Yamanaka et al. (1999, manuscript submitted to *J. Phys. Oceanogr.*).

There have been several schemes developed that have little numerical dispersion and a higher order of accuracy compared with the centered differencing scheme. One of the most accurate schemes to date is the flux-corrected transport (FCT) scheme of Boris and Book (1973). When the FCT scheme is incorporated into OGCMs, computational cost doubles compared with models with the centered differencing or the upstream scheme (Gerdes et al. 1991). There are some less expensive alternatives: the Uniformly Third-Order Polynomial Interpolation Algorithm (UTOPIA; Leonard et al. 1993) and the Multidimensional Positive Definite Advection Transport Algorithm (MPDATA; Smolarkiewicz 1984). They have the same or higher order of accuracy as compared with the centered differencing scheme, and exhibit little numerical dispersion.

Corresponding author address: Dr. Hiroyasu Hasumi, Center for Climate System Research, University of Tokyo, 4-6-1 Komaba, Meguro-ku, Tokyo 153-8904, Japan.
E-mail: hasumi@ccsr.u-tokyo.ac.jp

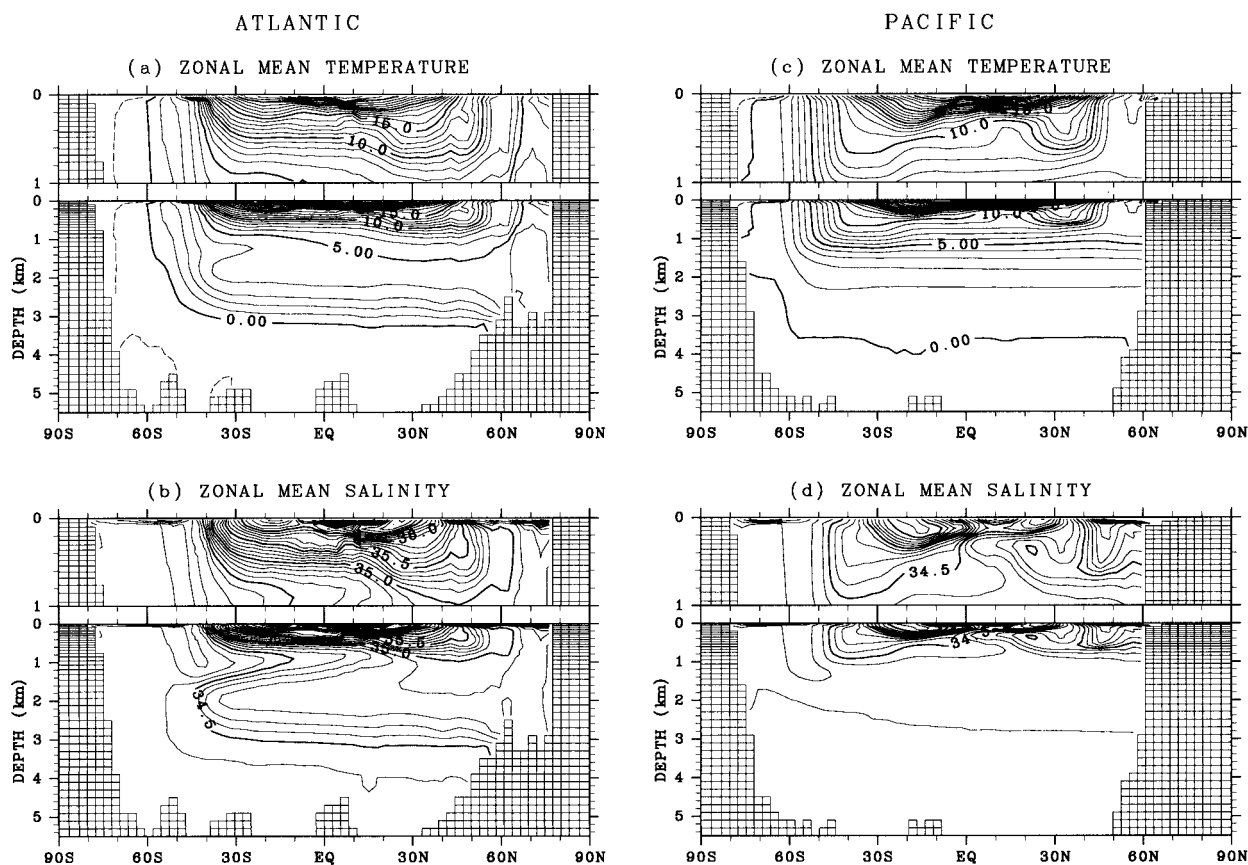


FIG. 1. Zonally averaged annual-mean distributions of (a) temperature and (b) salinity in the Atlantic and (c) temperature and (d) salinity in the Pacific for the case UTOPIA. Contour interval is 1°C for temperature and 0.1 psu for salinity.

UTOPIA (and its associate schemes) and MPDATA have already been applied to some OGCM-based studies, but applicability of them to realistic ocean simulation has not been well discussed. Farrow and Stevens (1995) incorporated the Quadratic Upstream Interpolation for Convective Kinematics (QUICK; Leonard 1979), which is one of the associated schemes of UTOPIA, into their OGCM for modeling the Southern Ocean. And they reported that under- and overshoot of the tracer values, which had been induced by numerical dispersion of the centered differencing scheme, were significantly reduced. Hecht et al. (1995) compared the performance of various advective transport schemes, including UTOPIA and MPDATA, in the context of two-dimensional passive tracer advection. They also compared computational costs of those schemes. Hecht et al. (1998) implemented those schemes in their OGCM with an idealized basin geometry and forcing and showed that dispersive error in the transport of temperature and salinity along the western boundary was much suppressed. Holland et al. (1998) chose QUICK as the tracer transport scheme in their global-domain OGCM and reported that the simulated tracer fields were improved.

In this study we incorporate UTOPIA and MPDATA, for both horizontal and vertical advection, into our

OGCM and then carry out simulations of the World Ocean circulation by using three schemes, the centered differencing scheme, UTOPIA, and MPDATA. The vertical eddy diffusion coefficient is chosen to be $1 \times 10^{-5} \text{ m}^2 \text{ s}^{-1}$. Results are compared with one another to assess usefulness of UTOPIA and MPDATA in reproducing observed features in the temperature and salinity fields at the thermocline depths. It is expected that such small vertical diffusivity as used here for the deep ocean causes too weak a circulation. Traditionally, vertical diffusivity has been taken higher for the deep ocean in OGCMs by simply prescribing it as a function of the depth (e.g., Bryan and Lewis 1979) or by assuming it to be a function of stability (e.g., Hirst and Cai 1994). Nevertheless, we do not adopt depth- or stability-dependent diffusivity. There is some evidence that vertical diffusivity in the deep ocean is spatially highly variable, and is as small as $1 \times 10^{-5} \text{ m}^2 \text{ s}^{-1}$ over smooth bottom topography (e.g., Polzin et al. 1997). Thus there is a need to check if the schemes behave reliably with such small vertical diffusivity in the deep ocean. For the model with UTOPIA, a case for larger vertical diffusivity is performed, and dependence on vertical diffusivity is also discussed.

The present paper is organized as follows. In section

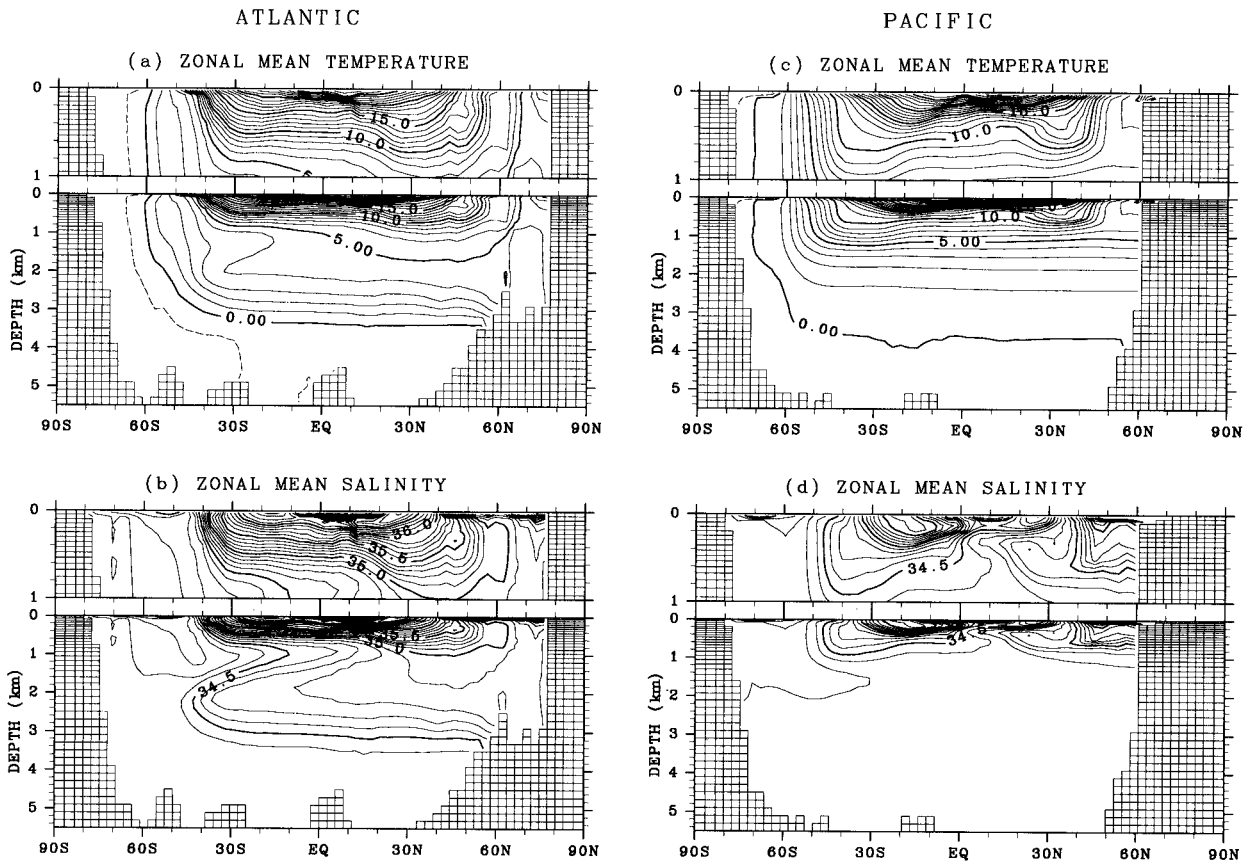


FIG. 2. Same as in Fig. 1 except for the case MPDATA.

2, the advection schemes used in this study are outlined. Model description and setup for the experiments are given in section 3. Results are described in section 4. Finally, summary and concluding remarks are presented in section 5.

2. Advective transport schemes for tracer

We briefly explain the concept of the advective transport schemes used herein. A good review is given by Rood (1987) for a variety of advective transport schemes and their characteristics.

For simplicity, let us consider the finite-difference discretization of a flux-form, one-dimensional advection equation for tracer ψ :

$$\frac{\partial \psi}{\partial t} = \frac{\partial}{\partial x}(u\psi), \quad (1)$$

where t is time, x is the spatial coordinate, and u is the advection velocity, which is assumed to be constant. When (1) is finite differenced in space with evenly spaced grid of width Δx , it becomes

$$\frac{\partial \psi_i}{\partial t} = \frac{u\psi_{i+1/2} - u\psi_{i-1/2}}{\Delta x} + \text{error}, \quad (2)$$

where the subscripts denote the spatial grid points. Values of ψ are defined and predicted at points of integer subscripts. Half integer value for the subscripts indicates the grid boundary between adjacent grids. The error depends on estimation of ψ at grid boundaries.

In the upstream scheme $\psi_{i-1/2}$ is estimated to be equal to the value of ψ at the grid point just upstream: $\psi_{i-1/2} = \psi_{i-1}$ for positive u and $\psi_{i-1/2} = \psi_i$ for negative u . In the centered differencing scheme $\psi_{i-1/2}$ is estimated by linear interpolation of the values of ψ at the grid points just up- and downstream: $\psi_{i-1/2} = (\psi_{i-1} + \psi_i)/2$. Accuracy in estimating $\psi_{i-1/2}$ is higher than that of the upstream scheme by one order.

Making use of ψ_i , ψ_{i-1} , and an additional gridpoint value of ψ in the upstream (ψ_{i-2} for positive u), we can estimate $\psi_{i-1/2}$ with quadratic interpolation. This method is named QUICK by Leonard (1979). The accuracy in the estimation of $\psi_{i-1/2}$ is higher by one order than that of the centered differencing scheme. Accuracy in solving (1) becomes higher when temporal variation in $\psi_{i-1/2}$ during the time step is taken into account. This method is named QUICKEST (QUICK with Estimated Streaming Terms) by Leonard (1979). Multidimensional application of QUICKEST, which is named UTOPIA, is given by Leonard et al. (1993), and flux-form imple-

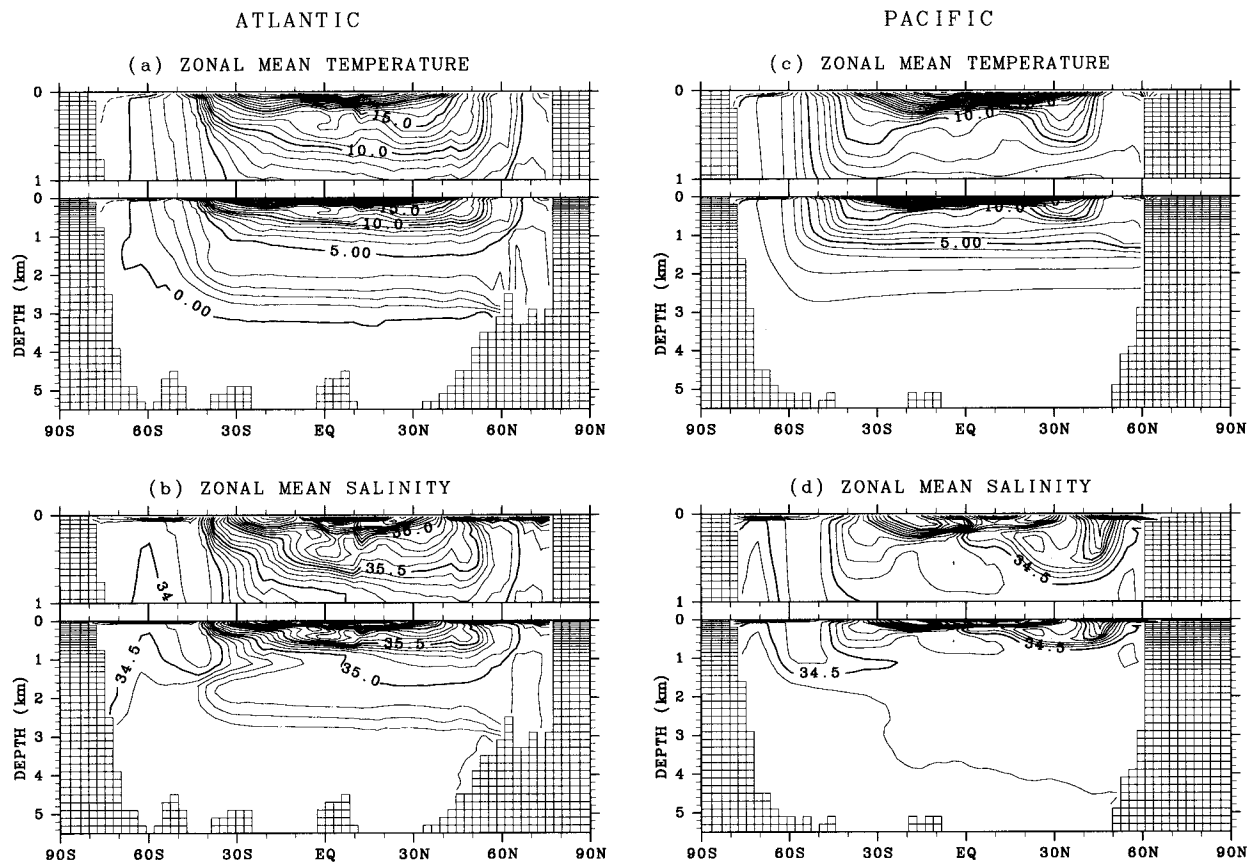


FIG. 3. Same as in Fig. 1 except for the case CTDIFF.

mentation of UTOPIA is documented by Leonard et al. (1994). In the application of UTOPIA to our OGCM, the horizontal dimension is separated from the vertical. That is, two-dimensional UTOPIA is used in the horizontal and QUICKEST is used in the vertical.

MPDATA (Smolarkiewicz 1984) is a flux-corrected transport scheme based on the upstream scheme. That is, time integration is first made by using the usual upstream scheme. Then, correction is made by use of the upstream scheme, where “anti-diffusive” velocity is applied instead of advective velocity. The anti-diffusive velocity is so defined that the numerical diffusion is corrected and that the procedure consequently ensures the same order of accuracy as the centered differencing scheme. The correction accompanies error, which can be reduced by iterative correction. By our experience in simulating the World Ocean, however, the iterative correction does not lead to notable improvement so that we only adopt single-time correction in the experiment presented herein. MPDATA requires that the advected quantity is positive everywhere. In this study, 10°C is added to temperature before calculating the advection and is subtracted afterward. We also tested the case where 5°C is used instead of 10°C , but there was no difference.

The schemes introduced here are based on an evenly

spaced grid. As described above, the estimate of ψ at grid boundaries by the centered differencing scheme and QUICKEST can be interpreted as interpolation. Thus, application of these schemes to an unevenly spaced grid is straightforward, and the order of accuracy is not lowered as long as variation in grid spacing is smaller than width of each grid itself by more than one order. For MPDATA, however, the anti-diffusive velocity cannot be well defined for unevenly spaced grid. It is possible to use the same formulation as developed for an evenly spaced grid, but the order of accuracy is lowered. The actual magnitude of error induced by uneven grid spacing depends on vertical velocity and difference between adjacent grids. The effect of uneven grid spacing is examined in an appendix.

3. Model description and setup for experiments

An OGCM used here is the CCSR-OGCM, which is a three-dimensional, rigid-lid ocean model developed at Center for Climate System Research (CCSR), University of Tokyo. The numerical schemes for other than advective tracer transport are similar to those described by Bryan (1969). Unstable stratification is removed by convective adjustment.

The model domain is global with realistic bathymetry.

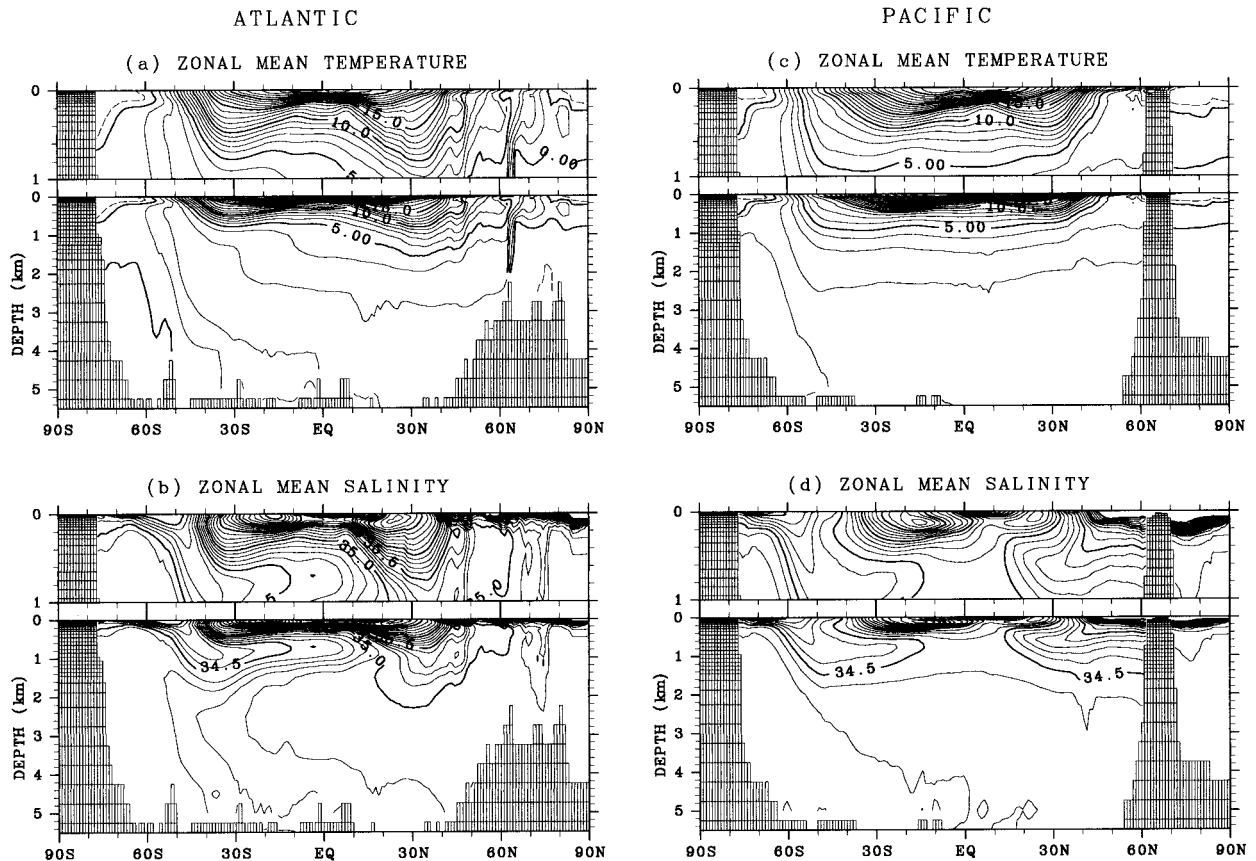


FIG. 4. Same as in Fig. 1 except for the climatology by Levitus and Boyer(1994) and Levitus et al. (1994).

For the sake of computational efficiency, the Arctic Ocean is completely removed. The Mediterranean Sea is also excluded. The horizontal resolution is about 2.8° both in the zonal and meridional directions. Such horizontal resolution as this is often categorized as “coarse,” in the sense that mesoscale eddies are not resolved. There are 40 levels in the vertical: the grid width is variable from 50 m for the top level to 200 m for the bottom level, containing 15 levels in the top 1000 m. Note that this vertical resolution is relatively high compared with other global ocean models. Isopycnal diffusion (Cox 1987) is applied, where the isopycnal eddy diffusion coefficient and the background horizontal eddy diffusion coefficient are chosen to be $1 \times 10^3 \text{ m}^2 \text{ s}^{-1}$ and $1 \times 10^2 \text{ m}^2 \text{ s}^{-1}$, respectively. The vertical eddy diffusion coefficient is $1 \times 10^{-5} \text{ m}^2 \text{ s}^{-1}$, unless otherwise noted. The coefficients for the vertical and the horizontal eddy viscosity are $1 \times 10^{-4} \text{ m}^2 \text{ s}^{-1}$ and $2.5 \times 10^5 \text{ m}^2 \text{ s}^{-1}$, respectively.

Wind forcing at the sea surface is taken from the monthly climatology of wind stress (Hellerman and Rosenstein 1983). Thermal and freshwater forcing at the sea surface is imposed by restoring to the monthly climatology of the sea surface temperature (Levitus and Boyer 1994) and salinity (Levitus et al. 1994). The re-

storing time constant is 30 days for both temperature and salinity.

Each model integration is initiated from a state of rest and constant temperature and salinity. Time integration is made until an almost steady state is obtained, approximately for 7000 years. The acceleration method of Bryan (1984) is adopted: the time step for the tracer equations is 1 day, and that for the momentum equations is a tenth of that for the tracer equations. Heat capacity is not modified for the acceleration. After an almost steady state is obtained, the integration is further continued for several tens of years without the acceleration method. Even when the forcing is seasonally varying, this procedure gives reasonable results with significantly reducing computational cost (Danabasoglu et al. 1996) although some systematic errors are expected (Nakano et al. 1999).

Experiments are carried out by using the three schemes presented in section 2. We call the cases by the names of the schemes: CTDIFF (centered differencing scheme), UTOPIA, and MPDATA. Another case is also calculated, where UTOPIA is adopted and the vertical eddy diffusion coefficient is taken to be $5 \times 10^{-5} \text{ m}^2 \text{ s}^{-1}$. We call this case UTOPIA-5.

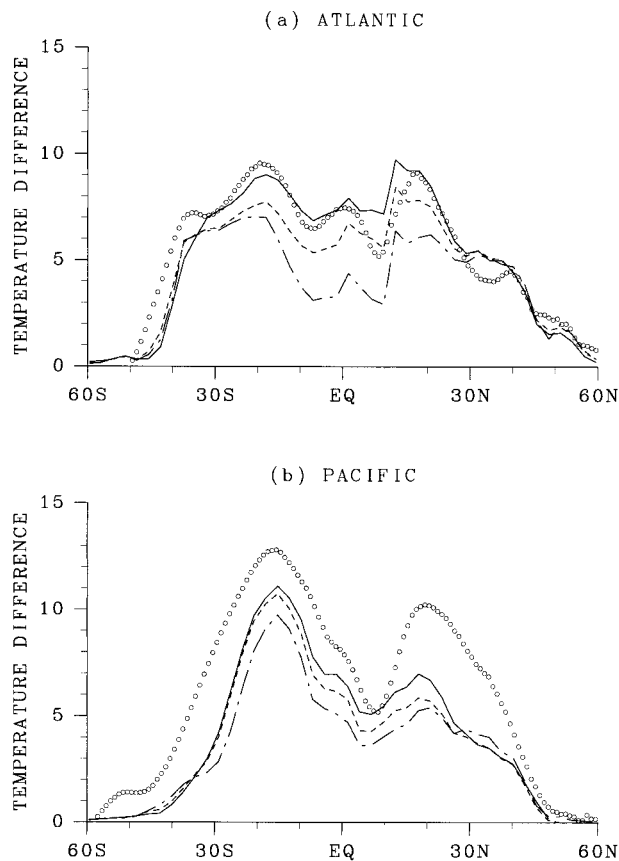


FIG. 5. Zonally averaged temperature difference ($^{\circ}\text{C}$) between the 200 and 600 m depths in the (a) Atlantic and (b) the Pacific. Solid line is for the case UTOPIA, dashed line for the case MPDATA, dash-and-dot line for the case CTDIFF, and circles for the climatology.

4. Results

Figures 1 through 3 show zonally averaged, annual-mean distributions of temperature and salinity in the Atlantic and the Pacific for the cases UTOPIA, MPDATA, and CTDIFF, respectively. For the sake of comparison, annual-mean climatology constructed from the temperature data of Levitus and Boyer (1994) and the salinity data of Levitus et al. (1994) is shown in Fig. 4.

As an index for sharpness of the thermocline, zonally averaged difference in temperature between depths 200 m and 600 m is plotted in Fig. 5. In the Atlantic, the thermocline is well simulated in the cases UTOPIA and MPDATA, while that in the case CTDIFF is diffuse, especially at low latitudes. The poor performance in the case CTDIFF is related to the irregular structure recognized in Fig. 3a. In the Pacific, the simulated thermocline is more diffuse in all of the cases than in the climatology. It is mainly due to the fact that the Pacific deep circulation is not reproduced in these experiments. This point is discussed later. Still, the thermocline for the cases UTOPIA and MPDATA is relatively sharp compared with that for the case CTDIFF.

The depth of the salinity minimum in the Atlantic, which corresponds to Antarctic Intermediate Water (AAIW), may be another good index to show the model's ability to simulate features at the thermocline depths. In the climatology (Fig. 4b), the depth is between 700 m and 800 m. In the cases UTOPIA and MPDATA (Figs. 1b and 2b), it is about 800 m. In the case CTDIFF (Fig. 3b), the northward intrusion of the salinity minimum is not well developed. Furthermore, there are many maxima and minima, particularly at low latitudes. The poor performance for the case CTDIFF is caused by dispersive error and associated artificial vertical mixing. The nonphysical, noisy structures due to the centered differencing seen in the temperature and salinity fields are better recognized in the horizontal view. Figure 6 shows horizontal distributions of the annual-mean salinity at the 175-m depth for the cases UTOPIA and CTDIFF. The distribution is smooth in the case UTOPIA, whereas it is irregular in the case CTDIFF because of under- or overshooting of tracer values. Such irregular structures are conspicuous where currents are strong, in the western boundary and the equatorial regions. Similar features are recognized in horizontal distributions of temperature. In previous studies with the centered differencing scheme, higher values were taken for vertical diffusivity to simulate the World Ocean. As a consequence, the tracer distribution does not look so irregular. However, the vertical diffusion coefficient of $1 \times 10^{-5} \text{ m}^2 \text{ s}^{-1}$ is too small to suppress nonphysical oscillation due to the centered differencing scheme.

The simulated deep or bottom water is colder and fresher, especially in the cases UTOPIA and MPDATA, than in the climatology. Since vertical diffusivity is taken very small even in the deep ocean, Antarctic Bottom Water (AABW), Circumpolar Deep Water, and accompanying circulations are not expected to be well reproduced in these simulations. Figure 7 shows the streamfunction of zonally integrated, annual-mean meridional overturning circulation in the Atlantic, the Pacific, and the global ocean for the cases UTOPIA, MPDATA, and CTDIFF. In the case CTDIFF, nonphysical structures are recognized. For example, there is downwelling to great depths in the subtropical Pacific. These structures are artifacts induced by numerical dispersion. In the cases UTOPIA and MPDATA, there is virtually no volume transport for the Atlantic bottom circulation and the Pacific deep circulation, and there is a middepth northward transport from the Southern Ocean to the subpolar North Pacific.

In the case UTOPIA, the intensity of the Atlantic deep circulation associated with southward extension of North Atlantic Deep Water is 17 Sv ($\text{Sv} \equiv 10^6 \text{ m}^3 \text{ s}^{-1}$) in its production region, with 13 Sv crossing the equator. The amount of the cross-equatorial transport is smaller than observational estimates (e.g., Schmitz 1995). This is mainly because we do not take special care to reproduce the Atlantic bottom circulation associated with the

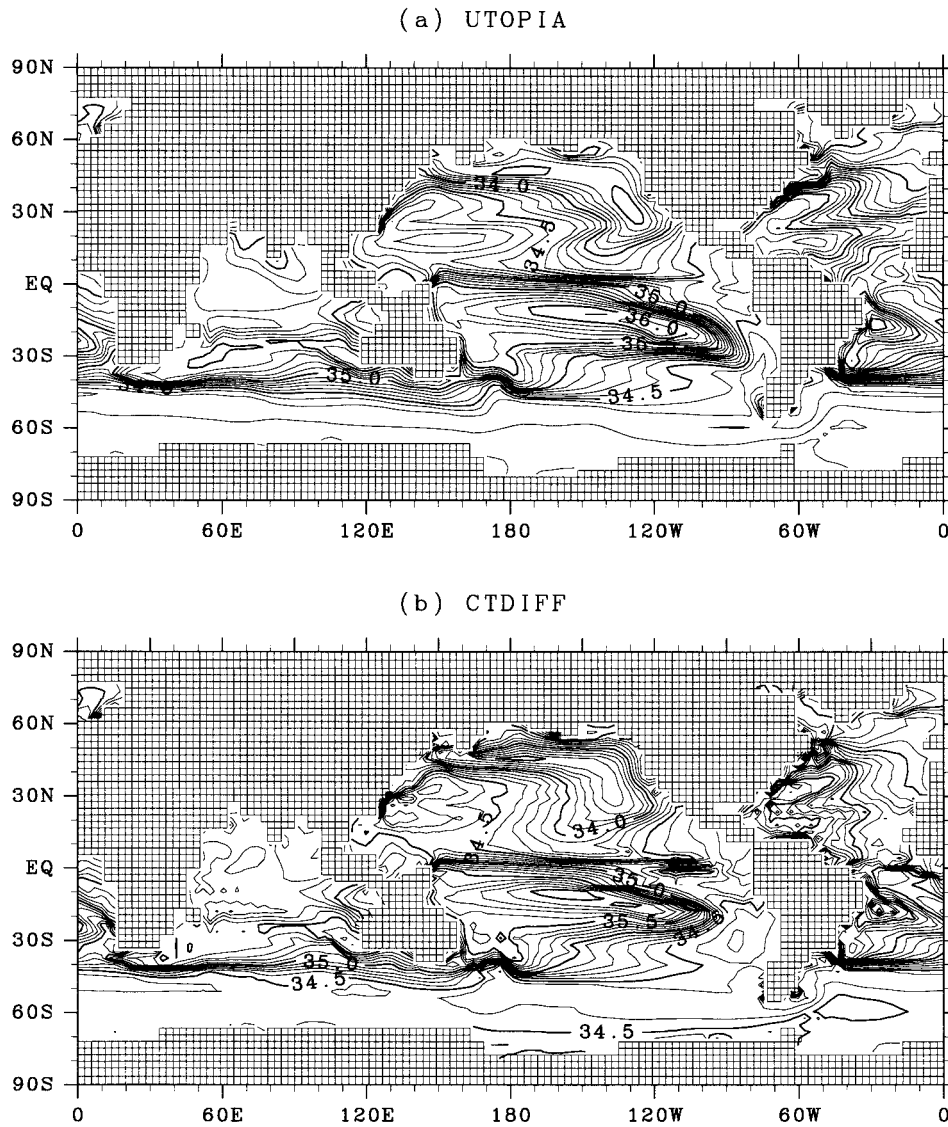


FIG. 6. Annual-mean salinity distribution at the 175-m depth for the cases (a) UTOPIA and (b) CTDIFF. Contour interval is 0.1 psu.

northward extension of AABW: adding 4 Sv to the Atlantic bottom circulation makes it closer to the observational estimates. The intensity of the circulation is similar in the case MPDATA. The slight difference between the cases UTOPIA and MPDATA may be a result of the different accuracy between UTOPIA and MPDATA, including the effect of unevenly spaced vertical grids. In these cases, the global meridional overturning circulation is mostly accounted for by the Atlantic deep circulation, as the Pacific deep circulation and the Atlantic bottom circulation are very weak. Thus, Figs. 7g and 7h indicate that most of the Atlantic deep circulation is connected to the upwelling in the Southern Ocean.

Figure 8 shows zonally averaged, annual-mean temperature and salinity distributions, and the streamfunction of zonally integrated, annual-mean meridional-

overturning circulation in the Atlantic and the Pacific for the case UTOPIA-5. Since the vertical diffusion coefficient is taken larger, $5 \times 10^{-5} \text{ m}^2 \text{ s}^{-1}$, the thermocline is more diffuse and the depth of AAIW in the Atlantic is deeper than in the case UTOPIA. Although reproduction of the thermocline is deteriorated, temperature and salinity of deep and bottom waters become closer to the climatology, and the Atlantic bottom circulation and the Pacific deep circulation are significantly intensified. The Pacific middepth northward transport seen in the case UTOPIA (Fig. 7d) now appears as the northward stretched upper circulation cell (Fig. 8f), as simulated in the Pacific model of Tsujino and Suginoara (1998). In order to reproduce well the Atlantic bottom circulation, the Pacific deep circulation, and also the thermocline, it is necessary to take into account the

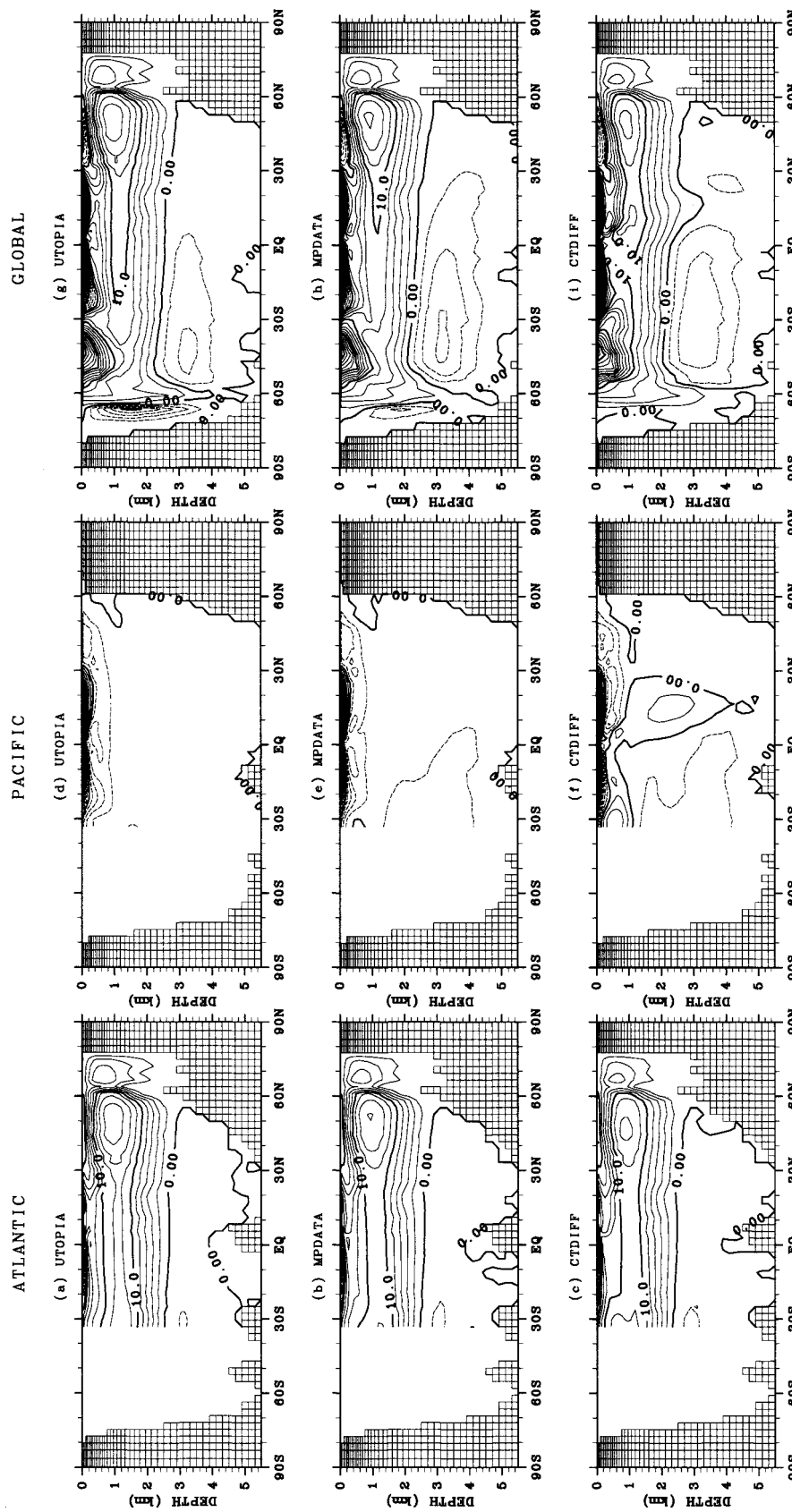


FIG. 7. Streamfunction of zonally integrated, annual-mean meridional overturning circulation in (a)–(c) the Atlantic, (d)–(f) the Pacific, and (g)–(i) the global ocean for the cases UTOPIA, MPDATA, and CTDIFF. Contour interval is 2 Sv.

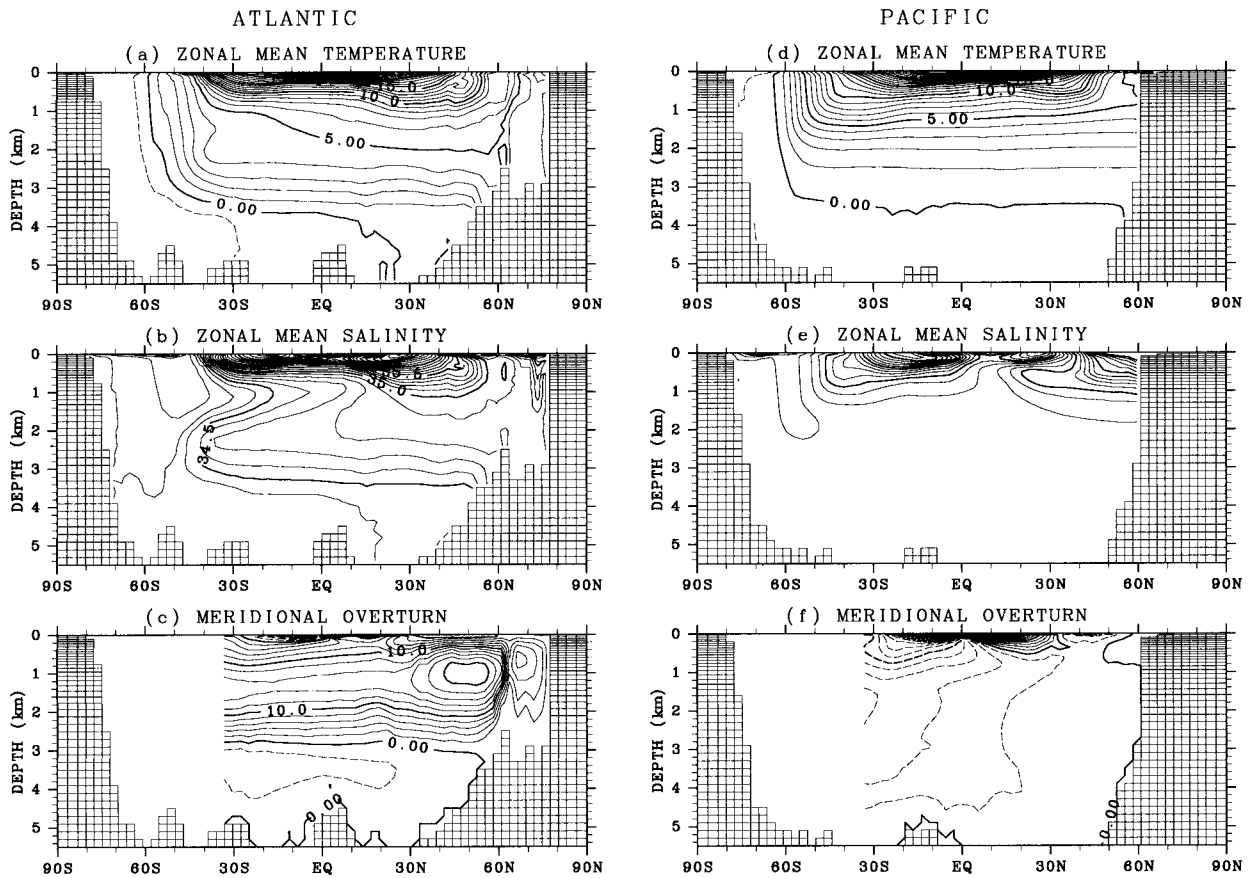


FIG. 8. Results of the case UTOPIA-5. Zonally averaged, annual-mean distributions of (a) temperature and (b) salinity, and (c) stream function of zonally integrated, annual-mean meridional overturning circulation in the Atlantic. (d)–(f) Same as (a)–(c) except for the Pacific. Contour interval is 1°C for temperature, 0.1 psu for salinity, and 2 Sv for stream function.

depth or stability dependence of vertical diffusivity (e.g., Bryan and Lewis 1979; Hirst and Cai 1994).

The production rate of NADW for the case UTOPIA-5 is 21 Sv, with 15 Sv crossing the equator, so that the Atlantic deep circulation is intensified by about 20% compared with the case UTOPIA. Scaling arguments and numerical experiments with idealized models (e.g., Marotzke 1997) indicate that intensity of the thermohaline meridional overturning is proportional to the two-thirds power of vertical diffusivity. According to this dependence, the circulation should be intensified by almost three times. This indicates that there is an important controlling factor for the intensity of the Atlantic deep circulation, which was not taken into account in such idealized experiments or scaling discussion. In such scaling arguments and idealized numerical experiments, upwelling is broadly distributed, as in the classical view of thermohaline circulation. On the other hand, the upwelling of the Atlantic deep circulation is confined in the Southern Ocean, as noted before. The concentrated upwelling is a manifestation of wind-enhanced thermohaline circulation (Tsuji and Sugihara 1999), that is, heating of deep water caused by

Ekman upwelling enhances thermohaline circulation with the upwelling confined there. Hasumi and Sugihara (1999) demonstrated that the Atlantic deep circulation is mostly accounted for by wind-enhanced thermohaline circulation and that heating in the Southern Ocean is a major controlling factor for intensity of the circulation.

5. Concluding remarks

In this study, two high-accuracy advective tracer transport schemes, UTOPIA and MPDATA, have been incorporated into an OGCM, and performance of them in simulating the World Ocean has been compared with that of the centered differencing scheme. For the vertical diffusion coefficient of $1 \times 10^{-5} \text{ m}^2 \text{ s}^{-1}$, which is consistent with observational estimates at the thermocline depths, the results of the present coarse resolution model show that UTOPIA and MPDATA ensure a reliable simulation at the thermocline depths whereas the centered differencing scheme does not. Computational cost increases only moderately with incorporating UTOPIA or MPDATA: the increase is less than 20% in our OGCM

compared with the model with the centered differencing scheme.

We emphasize the importance of applying a good advection scheme not only for the vertical direction but also for the horizontal. The horizontal advection also induces numerical dispersion for the centered differencing scheme and numerical diffusion for the upstream scheme. These effects become serious where the horizontal velocity is large, for example, over irregular topography or in the western boundary region (e.g., Farrow and Stevens 1995). To accomplish a reliable simulation in those regions, the centered differencing or the upstream scheme is not sufficient. In addition, adoption of the eddy-induced tracer transport scheme by Gent and McWilliams (1990) also makes it necessary to use a good advection scheme in the horizontal, as their parameterization works to enhance advective velocity (Weaver and Eby 1997).

For the vertical diffusivity of $1 \times 10^{-5} \text{ m}^2 \text{ s}^{-1}$ with UTOPIA or MPDATA, the Atlantic bottom circulation associated with the northward extension of AABW and the Pacific deep circulation associated with the northward extension of CDW are not reproduced at all. The experiment for the vertical diffusivity of $5 \times 10^{-5} \text{ m}^2 \text{ s}^{-1}$ with UTOPIA indicates that much higher diffusivity than $1 \times 10^{-5} \text{ m}^2 \text{ s}^{-1}$ is required for the existence of the Atlantic bottom circulation and the Pacific deep circulation. Taking into consideration that the thermocline is well reproduced for the vertical diffusivity of $1 \times 10^{-5} \text{ m}^2 \text{ s}^{-1}$, there should be significant depth dependence in vertical diffusivity. It is also known that there is strong spatial variations in vertical diffusivity in the deep ocean (e.g., Polzin et al. 1997). In regard to incorporating horizontal inhomogeneity of vertical diffusivity in the deep ocean into OGCMs, too, a good advection scheme is necessary, as there are regions of very small vertical diffusivity. There is an attempt to study the effects of inhomogeneous vertical diffusivity on the World Ocean circulation by using an OGCM with UTOPIA (Hasumi and Sugimoto 1999, manuscript submitted to *J. Geophys. Res.*). The Atlantic deep circulation is not much affected by vertical diffusivity because its intensity is controlled by the heating caused by the Ekman upwelling in the Southern Ocean (Hasumi and Sugimoto 1999).

Acknowledgments. We are thankful to W. R. Holland for sharing his experiences on the numerical schemes with us. Discussions with R. Furue, H. Tsujino, and M. Miki were very helpful. Comments from two anonymous reviewers were helpful to improve our manuscript.

APPENDIX

Effect of Uneven Grid Spacing for MPDATA

To evaluate the effect of uneven grid spacing for MPDATA, we make a sensitivity test. The one dimen-

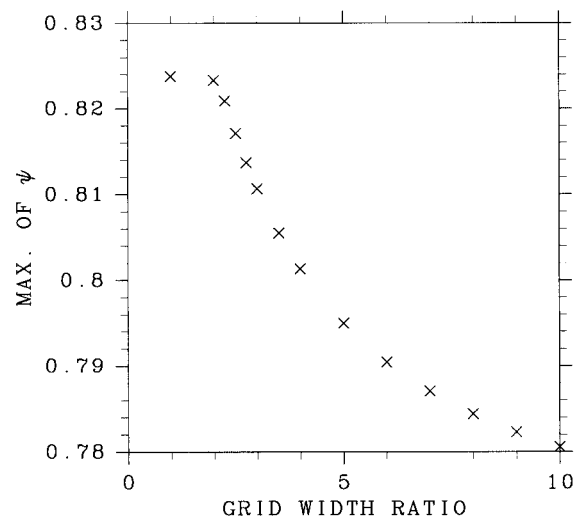


FIG. A1. Maximum value of ψ at the end of the integration plotted against the ratio of the largest grid width to the smallest one.

sional advection equation (1) is numerically solved with MPDATA. All the variables are regarded as nondimensional quantities. The advection velocity u is taken constant at 1. The region is $0 \leq x \leq 1$, and the cyclic boundary condition is imposed. The region is divided into 50 computational grids of variable width. The grid width is largest at the center of the region, is smallest at the boundaries, and varies linearly.

Starting from $\psi = \exp[-100 \times (x - \frac{1}{2})^2]$ at $t = 0$, the model is integrated until $t = 1$ with the time step of 0.01. Maximum value of ψ at the end of the integration (located at the center of the domain) is plotted against the ratio of the largest grid width to the smallest one in Fig. A1. The error drastically increases when the ratio exceeds 2. The vertical grid width variation of the OGCM used in this study approximately corresponds to the ratio of 4. The same experiment is made for the upstream scheme on the evenly spaced grid. The resulting maximum value of ψ is 0.456, which is much less than in any case shown in Fig. A1.

REFERENCES

- Boris, J. P., and D. L. Book, 1973: Flux-corrected transport, I, SHAST: A fluid transport algorithm that works. *J. Comput. Phys.*, **11**, 38–69.
- Bryan, K., 1969: A numerical method for the study of the circulation of the world ocean. *J. Comput. Phys.*, **4**, 347–376.
- , 1984: Accelerating the convergence to equilibrium of ocean climate models. *J. Phys. Oceanogr.*, **14**, 666–673.
- , and L. J. Lewis, 1979: A water mass model of the world ocean. *J. Geophys. Res.*, **84**, 2503–2517.
- Cox, M. D., 1987: Isopycnal diffusion in a z -coordinate ocean model. *Ocean Modelling* (unpublished manuscripts), **74**, 1–5.
- Danabasoglu, G., J. C. McWilliams, and W. G. Large, 1996: Approach to equilibrium in accelerated global oceanic models. *J. Climate*, **9**, 1092–1110.
- Farrow, D. E., and D. P. Stevens, 1995: A new tracer advection scheme for Bryan and Cox type ocean general circulation models. *J. Phys. Oceanogr.*, **25**, 1731–1741.

- Gent, P. R., and J. C. McWilliams, 1990: Isopycnal mixing in ocean circulation models. *J. Phys. Oceanogr.*, **20**, 150–155.
- Gerdes, R., C. Köberle, and J. Willebrand, 1991: The influence of numerical advection schemes on the results of ocean general circulation models. *Climate Dyn.*, **5**, 211–226.
- Gregg, M. C., 1989: Scaling turbulent dissipation in the thermocline. *J. Geophys. Res.*, **94**, 9686–9698.
- Hasumi, H., and N. Sugimoto, 1999: Atlantic deep circulation controlled by heating in the Southern Ocean. *Geophys. Res. Lett.*, in press.
- Hecht, M. W., W. R. Holland, and P. J. Rasch, 1995: Upwind-weighted advection schemes for ocean tracer transport: An evaluation in a passive tracer context. *J. Geophys. Res.*, **100**, 763–778.
- , F. O. Bryan, and W. R. Holland, 1998: A consideration of tracer advection schemes in a primitive equation ocean model. *J. Geophys. Res.*, **103**, 3301–3321.
- Hellerman, S., and M. Rosenstein, 1983: Normal monthly wind stress over the world ocean with error estimates. *J. Phys. Oceanogr.*, **13**, 1093–1104.
- Hirst, A. C., and W. Cai, 1994: Sensitivity of a world ocean GCM to changes in subsurface mixing parameterization. *J. Phys. Oceanogr.*, **24**, 1256–1279.
- Holland, W. R., J. C. Chow, and F. O. Bryan, 1998: Application of a third-order upwind scheme in the NCAR ocean model. *J. Climate*, **11**, 1487–1493.
- Ledwell, J. R., A. J. Watson, and C. S. Law, 1993: Evidence for slow mixing across the pycnocline from an open-ocean tracer-release experiment. *Nature*, **364**, 701–703.
- Leonard, B. P., 1979: A stable and accurate convective modelling procedure based on quadratic upstream interpolation. *Comput. Method Appl. Mech. Eng.*, **19**, 59–98.
- , M. K. MacVean, and A. P. Lock, 1993: Positivity-preserving numerical schemes for multidimensional advection. NASA Tech. Memo. 106055, ICOMP-93-05, 62 pp. [Available from National Aeronautical and Space Administration, Washington, DC 20546-0001.]
- , —, and —, 1994: The flux-integral method for multidimensional convection and diffusion. NASA Tech. Memo. 106679, ICOMP-94-13., 27 pp. [Available from National Aeronautical and Space Administration, Washington, DC 20546-0001.]
- Levitus, S., and T. P. Boyer, 1994: *World Ocean Atlas 1994*. Vol. 4: *Temperature*, U.S. Department of Commerce, 117 pp.
- , R. Burgett, and T. P. Boyer, 1994: *World Ocean Atlas 1994*. Vol. 3: *Salinity*, U.S. Department of Commerce, 99 pp.
- Maier-Reimer, E., U. Mikolajewicz, and K. Hasselmann, 1993: Mean circulation of the Hamburg LSG OGCM and its sensitivity to the thermohaline surface forcing. *J. Phys. Oceanogr.*, **23**, 731–757.
- Marotzke, J., 1997: Boundary mixing and the dynamics of three-dimensional thermohaline circulation. *J. Phys. Oceanogr.*, **27**, 1713–1728.
- Nakano, H., R. Furue, and N. Sugimoto, 1999: Effect of seasonal forcing on global circulation in a world ocean general circulation model. *Climate Dyn.*, in press.
- Polzin, K. L., J. M. Toole, J. R. Ledwell, and R. W. Schmitt, 1997: Spatial variability of turbulent mixing in the abyssal ocean. *Science*, **276**, 93–96.
- Rood, R. B., 1987: Numerical advection algorithms and their role in atmospheric transport and chemistry models. *Rev. Geophys.*, **25**, 71–100.
- Schmitz, W. J., Jr., 1995: On the interbasin-scale thermohaline circulation. *Rev. Geophys.*, **33**, 151–173.
- Smolarkiewicz, P. K., 1984: A fully multidimensional positive definite advection transport algorithm with small implicit diffusion. *J. Comput. Phys.*, **54**, 325–362.
- Sugimoto, N., and S. Aoki, 1991: Buoyancy-driven circulation as horizontal convection on beta-plane. *J. Mar. Res.*, **49**, 295–320.
- Tsujino, H., and N. Sugimoto, 1998: Thermohaline effects on upper layer circulation of the North Pacific. *J. Geophys. Res.*, **103**, 18 665–18 679.
- , and —, 1999: Thermohaline circulation enhanced by wind forcing. *J. Phys. Oceanogr.*, **29**, 1506–1516.
- Weaver, A. J., and M. Eby, 1997: On the numerical implementation of advection schemes for use in conjunction with various mixing parameterization in the GFDL ocean model. *J. Phys. Oceanogr.*, **27**, 369–377.